

Supporting Information:

Harnessing multifunctional collagen mimetic peptides to create bioinspired stimuli responsive hydrogels for controlled cell culture

Eden M. Ford^{1#}, Amber M. Hilderbrand^{1#}, April M. Kloxin^{1,2*}

¹Department of Chemical and Biomolecular Engineering, University of Delaware, Newark DE 19716 USA

²Department of Materials Science and Engineering, University of Delaware, Newark DE 19716 USA

#Authors contributed equally to this work

*Corresponding Author Email: akloxin@udel.edu

Table of Contents

| | |
|---|----|
| Supplemental Figures..... | 3 |
| Figure S1: mfCMP liquid chromatography tandem mass spectrometry..... | 3 |
| Figure S2: Circular dichroism of mfCMP in water and sodium phosphate..... | 4 |
| Figure S3: Fibrillar assembly of mfCMP in different buffers | 5 |
| Figure S4: Physically crosslinked mfCMP hydrogels assembled in sodium phosphate buffer and material response to increased strain..... | 5 |
| Figure S5: Polymer 4-arm PEG-SH ¹ H NMR | 6 |
| Figure S6: Photoinitiator LAP ¹ H NMR..... | 7 |
| Figure S7: Non-assembling linker peptide mass spectrometry | 7 |
| Figure S8: TEM of lyophilized and resuspended mfCMP | 8 |
| Figure S9: <i>In situ</i> composite hydrogel response to increased strain..... | 9 |
| Figure S10: <i>In situ</i> characterization of physically assembled harvested collagen hydrogel mechanical properties | 10 |
| Figure S11: <i>In situ</i> harvested collagen hydrogel response to increased strain | 10 |
| Figure S12: Thermoresponsive properties of mfCMP-PEG hybrid hydrogels..... | 11 |
| Figure S13: Integrin-binding pendent peptide mass spectrometry | 11 |
| Figure S14: Equilibrium swollen hydrogel mechanical properties under physiologically relevant conditions | 12 |
| Figure S15: Human lung fibroblast viability in mfCMP-RGDS-PEG hydrogel 24 hours after encapsulation | 12 |
| Figure S16: Impact of mfCMP-RGDS-PEG hydrogels on human lung fibroblast shape factor (sphericity)..... | 13 |
| Figure S17: Number of cells per cluster of human lung fibroblasts in response to mfCMP- RGDS-PEG hydrogels | 13 |
| Figure S18: Total distance traveled and displacement of human lung fibroblasts in response to mfCMP-RGDS-PEG hydrogels..... | 14 |
| Figure S19: Impact of mfCMP-RGDS-PEG hydrogels on human lung fibroblast motility | 14 |
| Supplemental Tables..... | 15 |
| Table S1: mfCMP-PEG hydrogel formulations | 15 |
| Table S2: mfCMP-RGDS-PEG hydrogel formulations for cell culture applications | 15 |
| Supplemental Videos | 16 |
| Video S1: Fibroblast motility in a 0% mfCMP hydrogel (0% of peptide linkages from mfCMP) | 16 |
| Video S2: Fibroblast motility in a 50% mfCMP hydrogel (50% of peptide linkages from mfCMP) | 16 |

Supplemental Figures

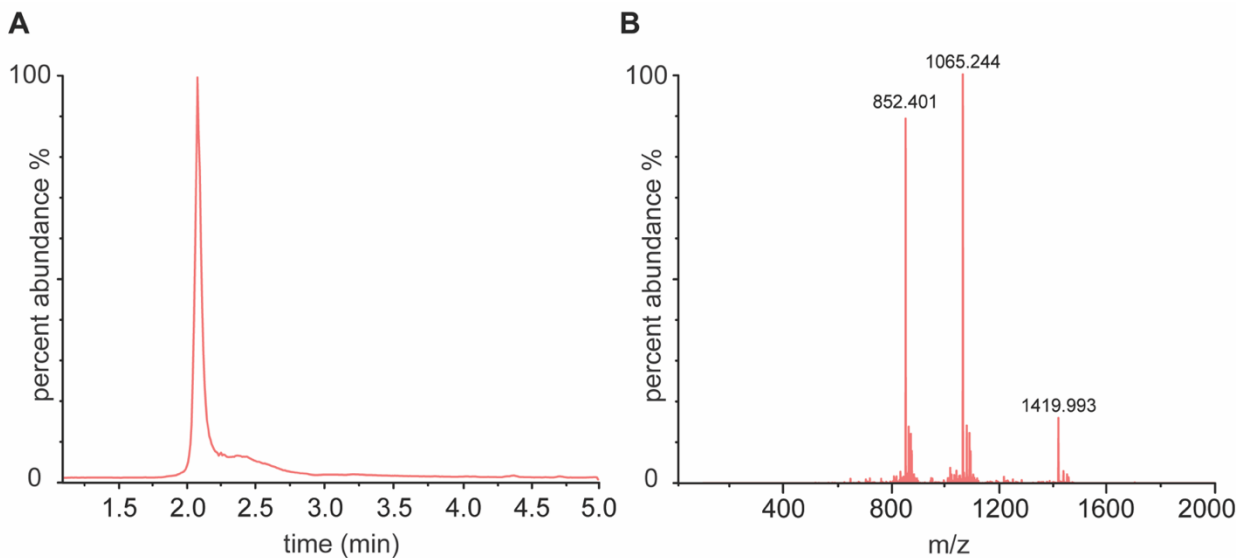


Figure S1: mfCMP liquid chromatography tandem mass spectrometry. Xevo G2-S QToF (XEVO) (A) UPLC trace and (B) electrospray ionization (ESI+) mass spectrometry of mfCMP [(PKG)₄PK(alloc)G(POG)₆(DOG)₄]. The desired product was observed with the expected molecular weight of 4256 g/mol ($[M+3H]^{3+} = 1420$ g/mol; $[M+4H]^{4+} = 1065$ g/mol; $[M+5H]^{5+} = 852$ g/mol).

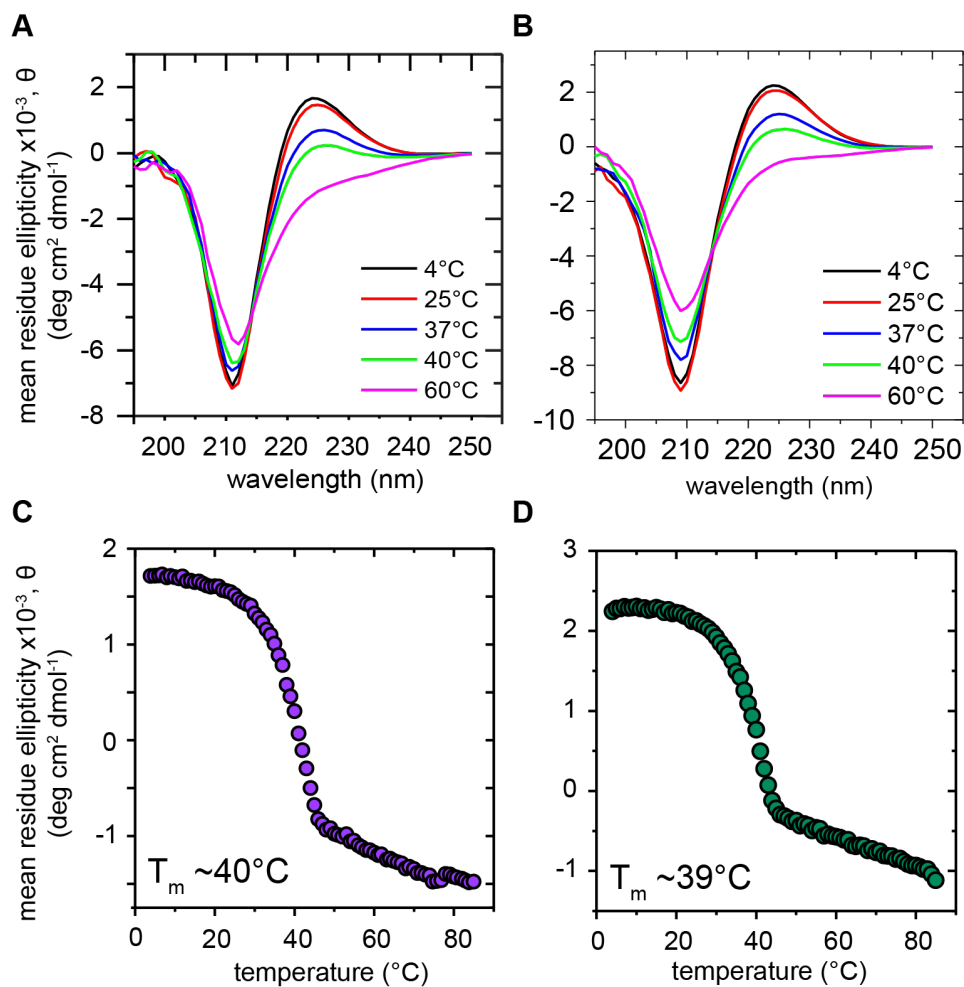
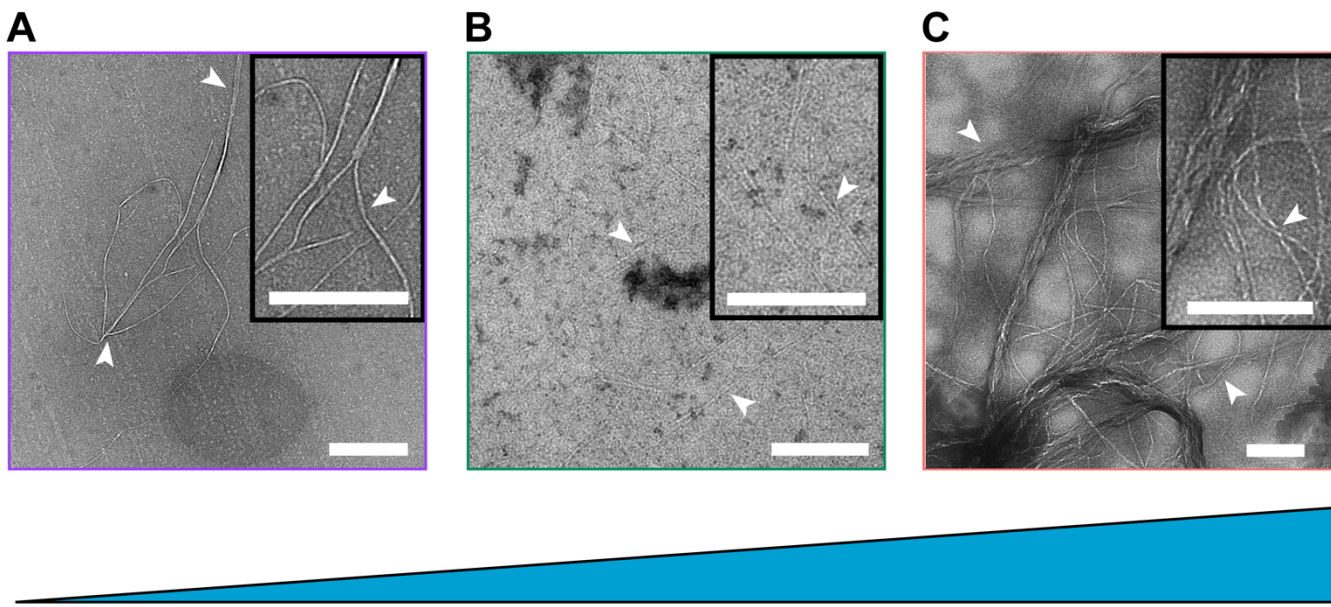


Figure S2: Circular dichroism of mfCMP in water and sodium phosphate. Wavelength scans of mfCMP (0.3 mM) in (A) DI water and (B) 10 mM sodium phosphate at designated temperatures with characteristic peak of a triple helix near 225 nm. ‘Melting’ (dissociation) of triple helices in (C) DI water and (D) 10 mM sodium phosphate was examined by monitoring mean residue ellipticity (MRE) at 222 nm during a temperature ramp from 4 °C to 85 °C, where the ‘melting’ temperature indicates where 50% of the triple helices are dissociated into individual peptide strands.



[salt]

Figure S3: Fibrillar assembly of mfCMP in different buffers. TEM images of mfCMP assembled for 48 hours at 1 mM in (A) DI H₂O, (B) 10 mM sodium phosphate, and (C) DPBS and diluted to 0.3 mM for casting onto the TEM grid followed by imaging; note, image shown in (C) is from main text **Figure 1D** to allow direct comparison here with (A) and (B)). (Arrows indicate a few of the fibrils in each image; Scale bars = 500 nm.)

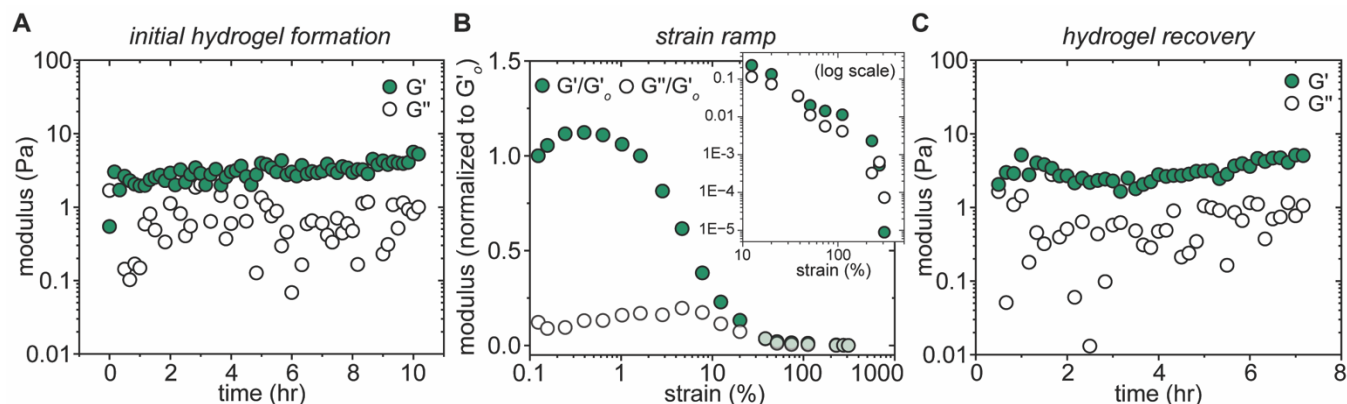


Figure S4: Physically crosslinked mfCMP hydrogels assembled in sodium phosphate buffer and material response to increased strain. (A) After melting at 85 °C a 5 mM mfCMP solution in 10 mM sodium phosphate was transferred to a temperature-controlled rheometer stage at 60 °C. The temperature was then ramped down to 25 °C over the course of 10 minutes, after which measurements were commenced at 0.1% strain and 1 rad/s. Gelation ($G' > G''$) was observed almost immediately upon cooling with good stability over the experiment time course. (B) mfCMP hydrogel response to a strain event (strain sweep 0.1-300%) showed an initial strain stiffening response (increase in G') followed by a decrease in modulus and deviation from linear viscoelastic behavior, where eventually $G'' > G'$ and $G'' \sim G'$ indicated liquid-like or near-liquid-like properties. (C) Physically assembled mfCMP were allowed to recover after the strain event, and recovery of gel-like properties ($G' > G''$) was observed with a return to the initial modulus within an hour with observation of a stable gel over the experimental time course.

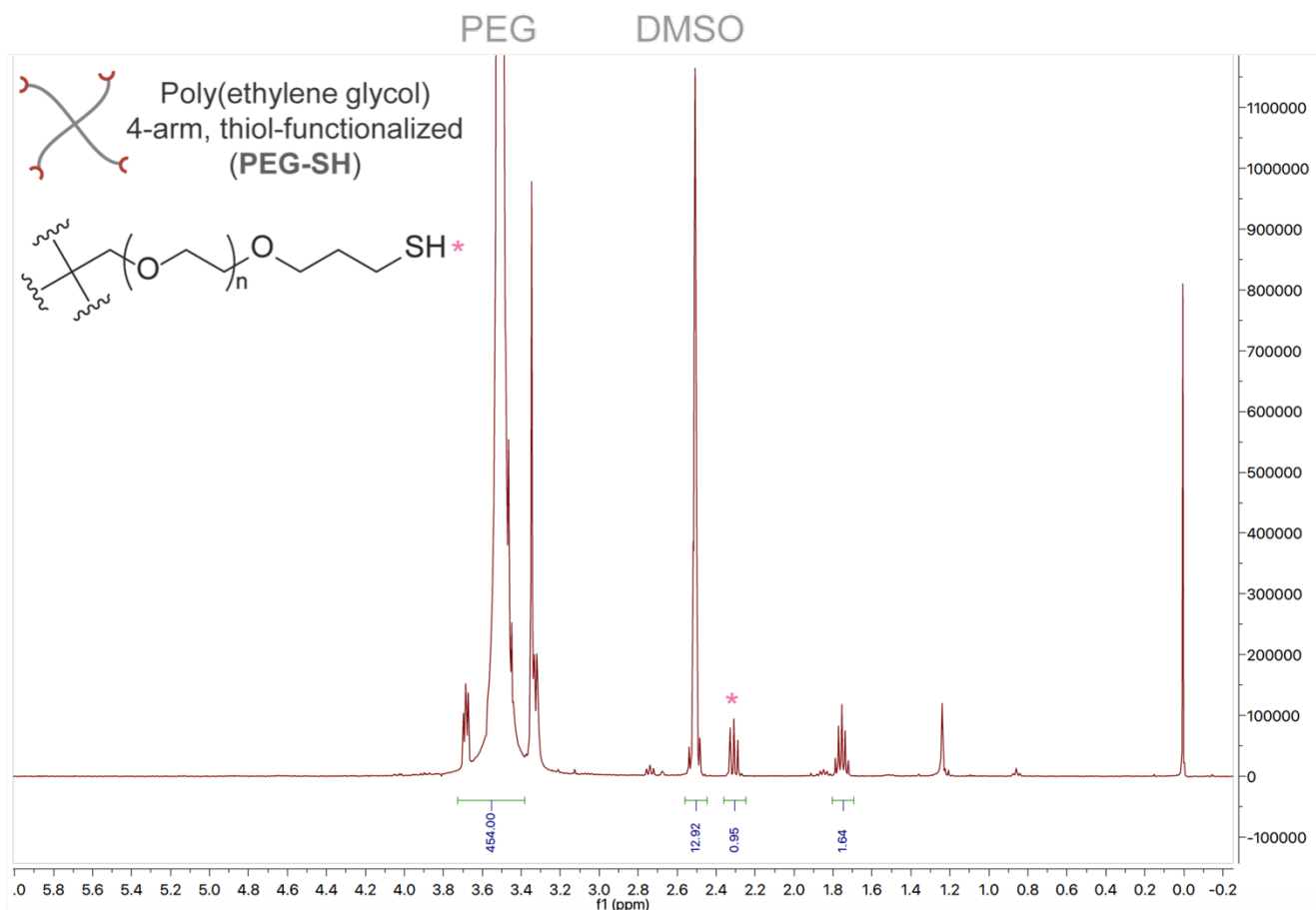


Figure S5: Polymer 4-arm PEG-SH ¹H NMR. ¹H NMR spectrum (400 MHz, DMSO-d₆) of 4-arm PEG ($M_n \sim 20$ kDa) functionalized with thiol end groups: 3.69 (s, 454H), 2.51 (d, 13H), 2.36-2.25 (m, 1H), 1.75 (p, 2H). The peak from ~ 3.75 to 3.35 ppm corresponds to the repeat units within the 4-arm PEG backbone and was assigned an integration value of 454H (number of protons associated with a single arm of the 4-arm 20 kDa PEG macromer). Integration of the thiol proton at 2.3 ppm was normalized to the integration of the PEG backbone protons to determine the functionality of thiols on the 4-arm PEG-SH, here 95%.

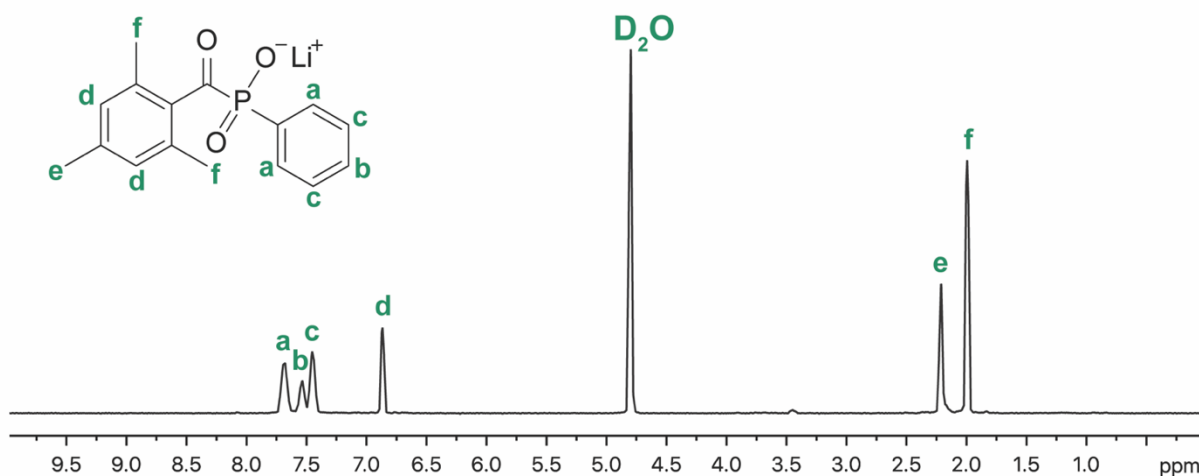


Figure S6: Photoinitiator LAP ¹H NMR. ¹H NMR spectrum (400 MHz, D₂O) of lithium phenyl-2,4,6-trimethylbenzoyl-phosphinate (LAP) photoinitiator. Protons and associated peaks are indicated.

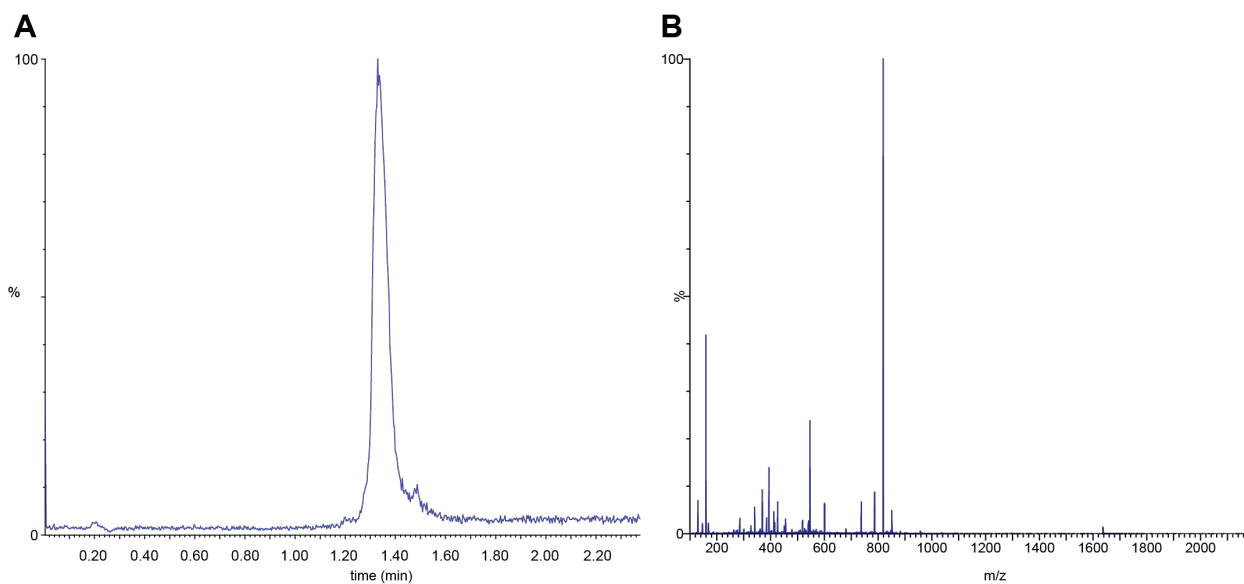


Figure S7: Non-assembling linker peptide mass spectrometry. Single Quadrupole Detector 2 (SQD2) (A) UPLC trace and (B) electrospray ionization (ESI+) mass spectrometry of the non-assembling, cell-degradable linker peptide [KK(alloc)GGPQG↓IWGQ GK(alloc)K]. The desired product was observed with the expected molecular weight of 1635 g/mol (Main peak: $[M+2H]^{2+} = 818$ g/mol).

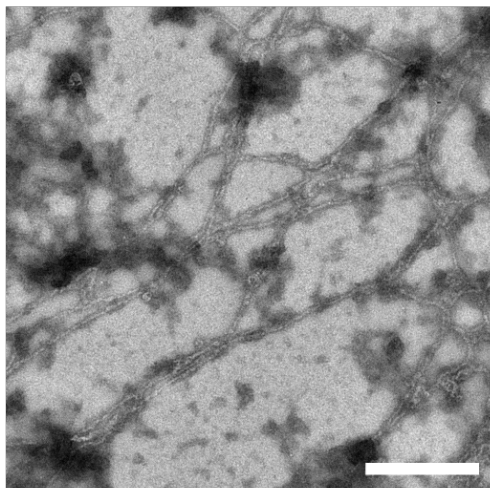


Figure S8: TEM of lyophilized and resuspended mfCMP. mfCMP was assembled at a concentration of 5 mM in DPBS, frozen at -80 °C, lyophilized, and resuspended in DPBS at a concentration of 1 mM for TEM.

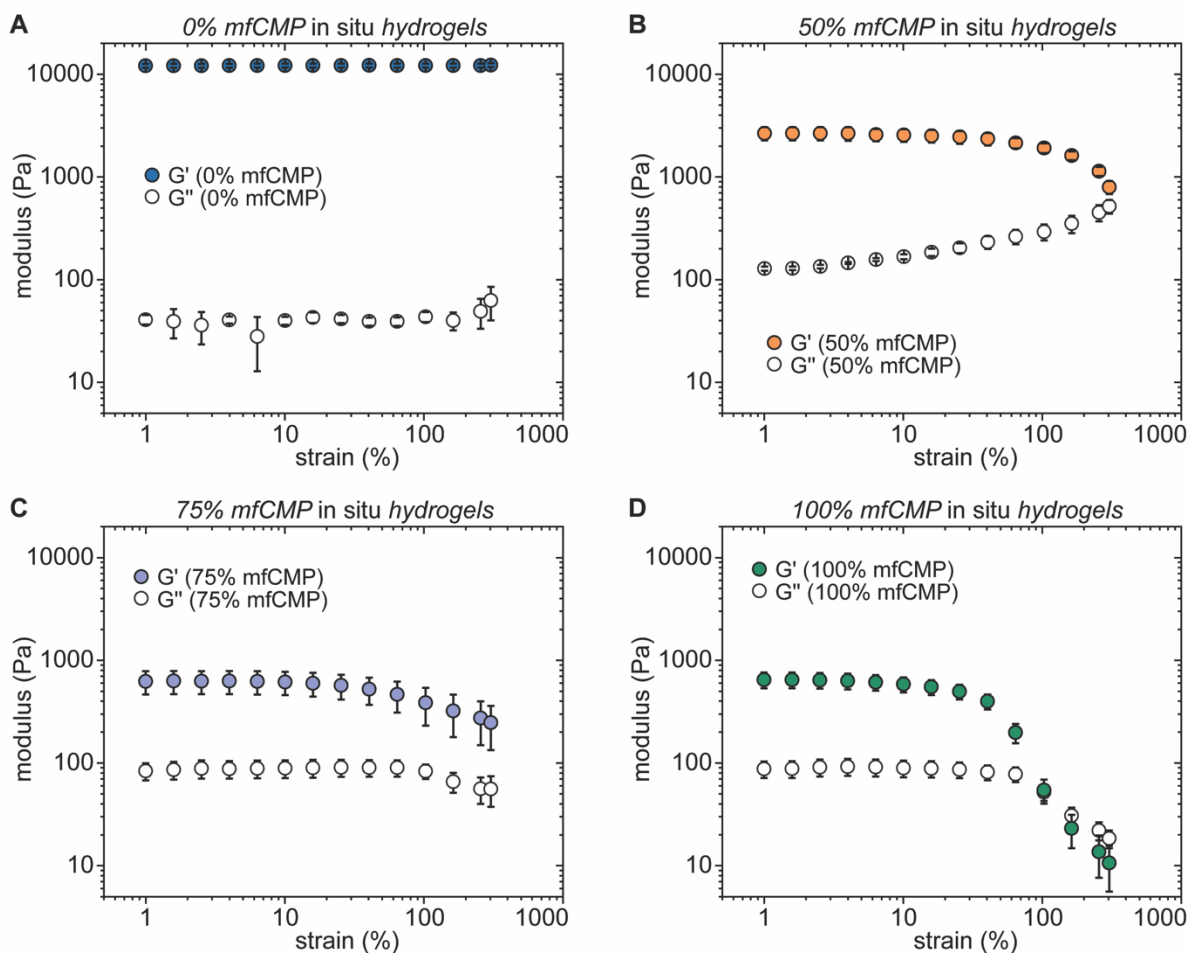


Figure S9: *In situ* composite hydrogel response to increased strain. Strain sweeps of *in situ*-formed hydrogels with increasing amounts of peptide linkages from mfCMPs at 25 °C ($n = 4$). Specifically, hydrogels contain (A) 0% mfCMP, (B) 50% mfCMP, (C) 75% mfCMP, and (D) 100% mfCMP. For most compositions, $G' > G''$ throughout the strain ramp, indicating that while strain-yielding was observed in some cases, the material remained in a gel-like state. However, when mfCMP peptide linkages were increased to 100% mfCMP (D), eventually $G'' > G'$ indicated liquid-like properties at high strain.

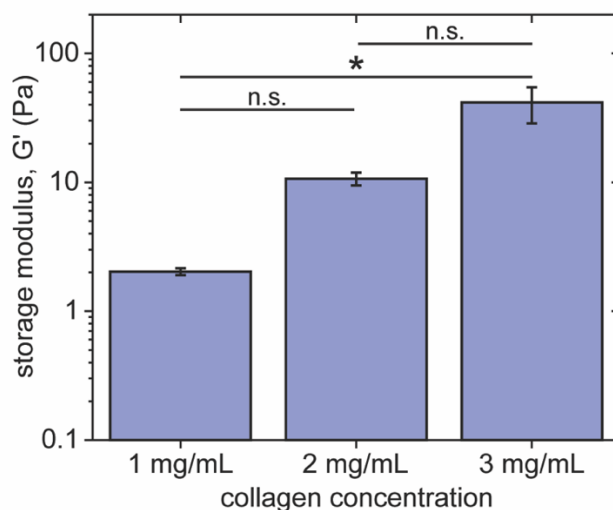


Figure S10: *In situ* characterization of physically assembled harvested collagen hydrogel mechanical properties. Average storage modulus of harvested collagen hydrogels formed with different concentrations of collagen I in DPBS (pH ~ 7) within the linear viscoelastic regime prior to conducting a strain experiment. (n = 3; * p < 0.05; n.s. = means are not significantly different.)

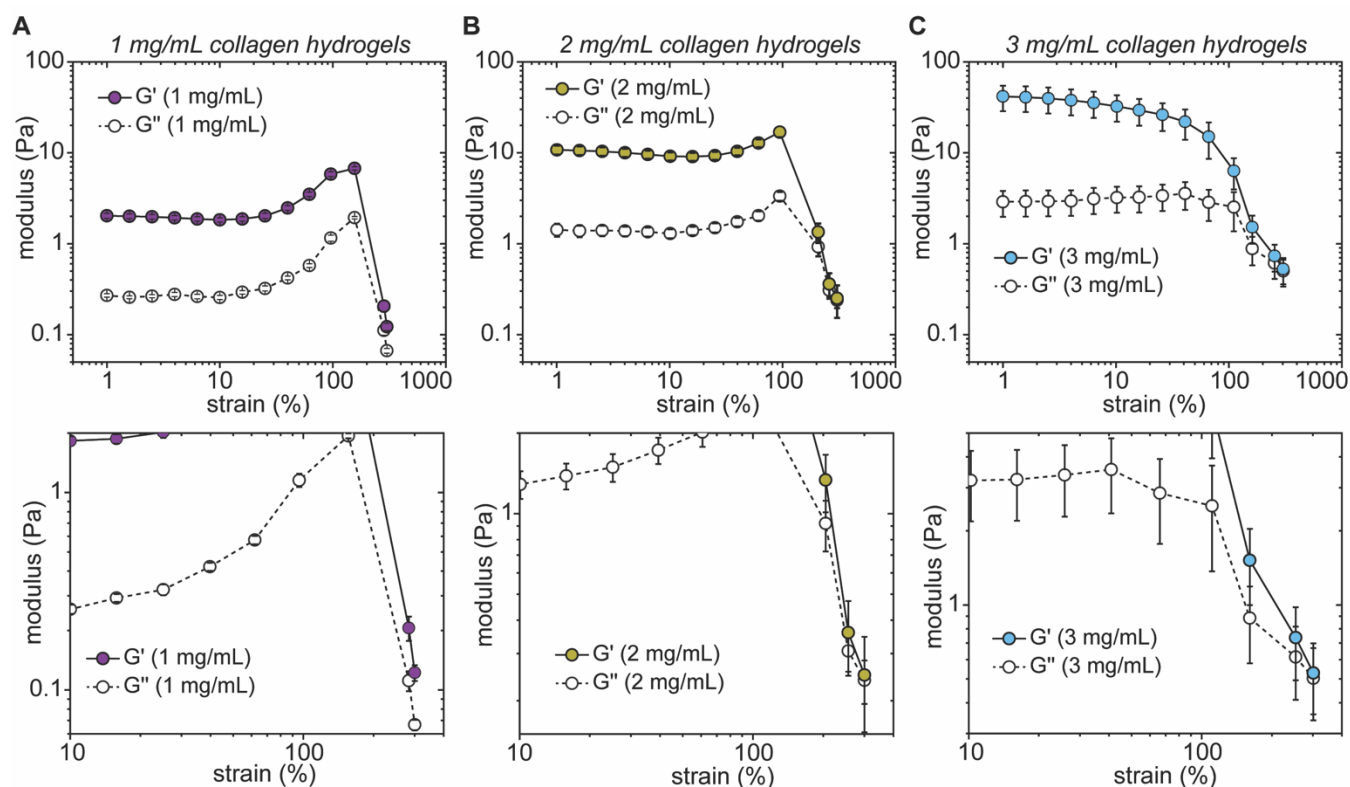


Figure S11: *In situ* harvested collagen hydrogel response to increased strain. Strain sweeps of *in situ*-formed assembled harvested collagen hydrogels with increasing collagen concentrations on the top row, with corresponding zoomed-in graphs on the bottom row (n = 3). Specifically, hydrogels contain (A) 1 mg/mL, (B) 2 mg/mL, or (C) 3 mg/mL collagen. At high strains, hydrogels undergo strain-softening and G' nears G'', indicating a tendency toward liquid-like properties at high strain.

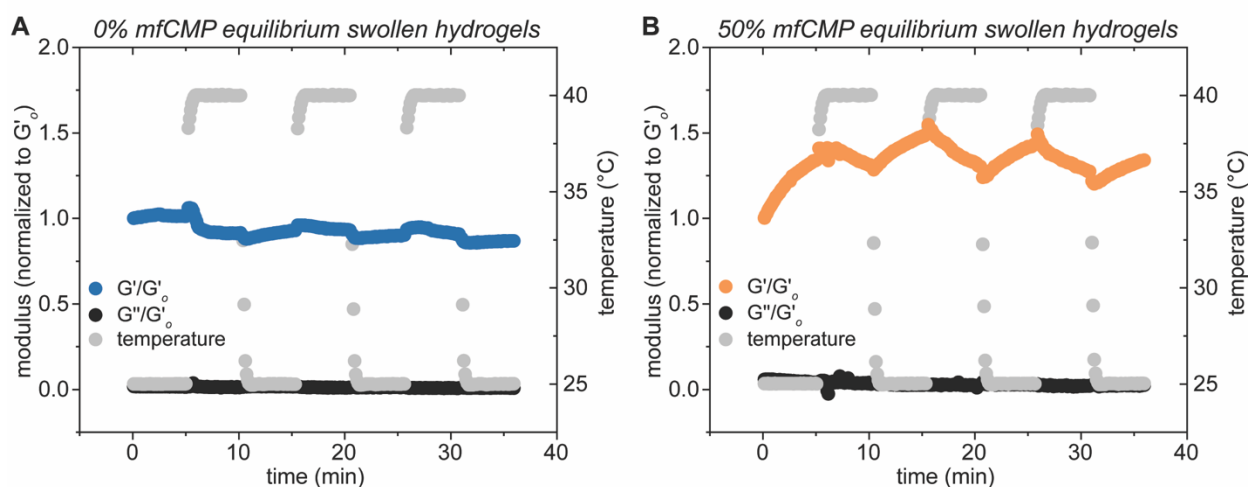


Figure S12: Thermoresponsive properties of mfCMP-PEG hybrid hydrogels. Equilibrium swollen hydrogels with (A) 0% mfCMP (control, 0 mM mfCMP) or (B) 50% mfCMP (10 mM mfCMP) were cycled between 25 °C and 40 °C while measuring the storage and loss modulus (normalized to the initial storage modulus for each condition). For both compositions, $G' > G''$ at all times, indicating that the hydrogels maintain gel-like properties over this temperature range. These data are presented in the main text (**Figure 3A**) and presented here on separate graphs for comparison between G' and G'' for each hydrogel.

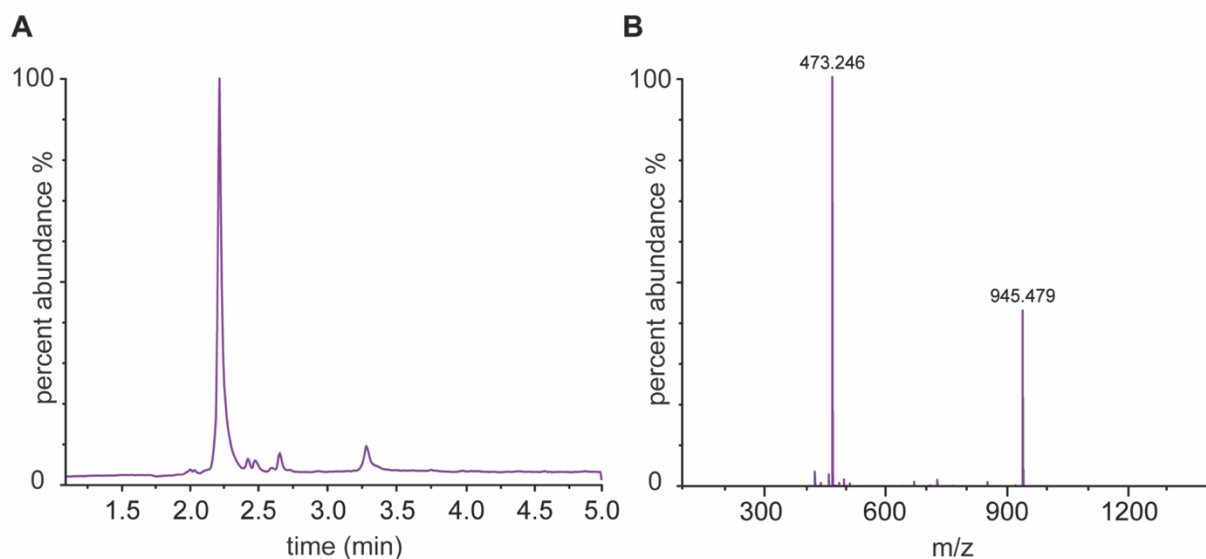


Figure S13: Integrin-binding pendent peptide mass spectrometry. Xevo G2-S QToF (XEVO) (A) UPLC trace and (B) electrospray ionization (ESI+) mass spectrometry of RGDS [K(alloc)GWGRRGDS]. The desired product was observed with the expected molecular weight of 945 g/mol ($[M+1H]^{1+} = 946$ g/mol; $[M+2H]^{2+} = 473$ g/mol).

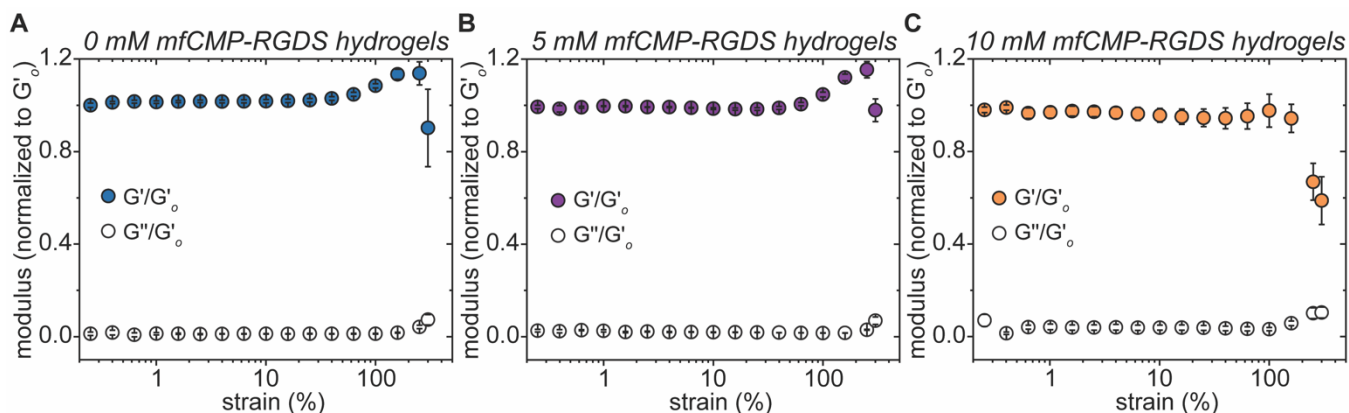


Figure S14: Equilibrium swollen hydrogel mechanical properties under physiologically relevant conditions. Strain sweeps of mfCMP-RGDS-PEG hydrogels with varying concentrations of mfCMP. Specifically, hydrogels contain (A) 0 mM mfCMP, (B) 5 mM mfCMP, and (C) 10 mM mfCMP, based on the mfCMP concentrations used to form the 0%, 25%, and 50% mfCMP-PEG hydrogel conditions, respectively. For all conditions, $G' > G''$ throughout the strain ramp, indicating that while strain-yielding was observed, the material remained in a gel-like state. (All measurements were performed at 37 °C after equilibrium swelling in DPBS (37 °C); $n = 4$.)

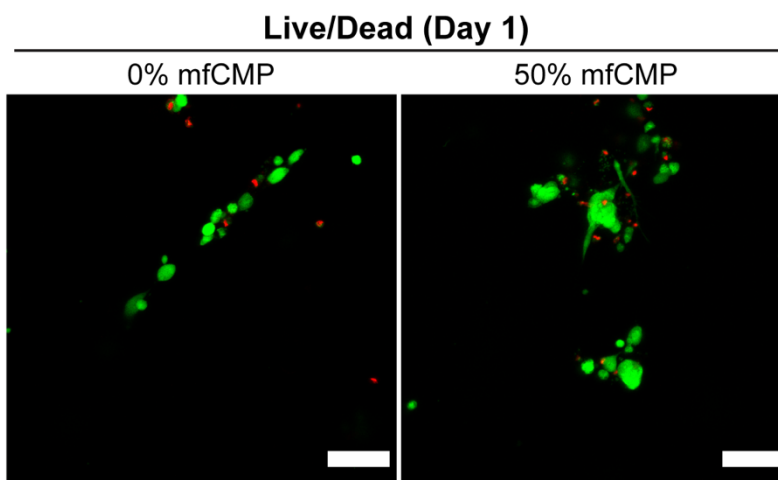


Figure S15: Human lung fibroblast viability in mfCMP-RGDS-PEG hydrogels 24 hours after encapsulation. Live/Dead staining (green = live cells; red = dead cell nuclei) of fibroblasts 24 hours after encapsulation within mfCMP-RGDS-PEG hydrogels with either 0% or 50% mfCMP (scale bars = 100 μm). Quantification of Live/Dead labeling is available in the main text (**Figure 5B**).

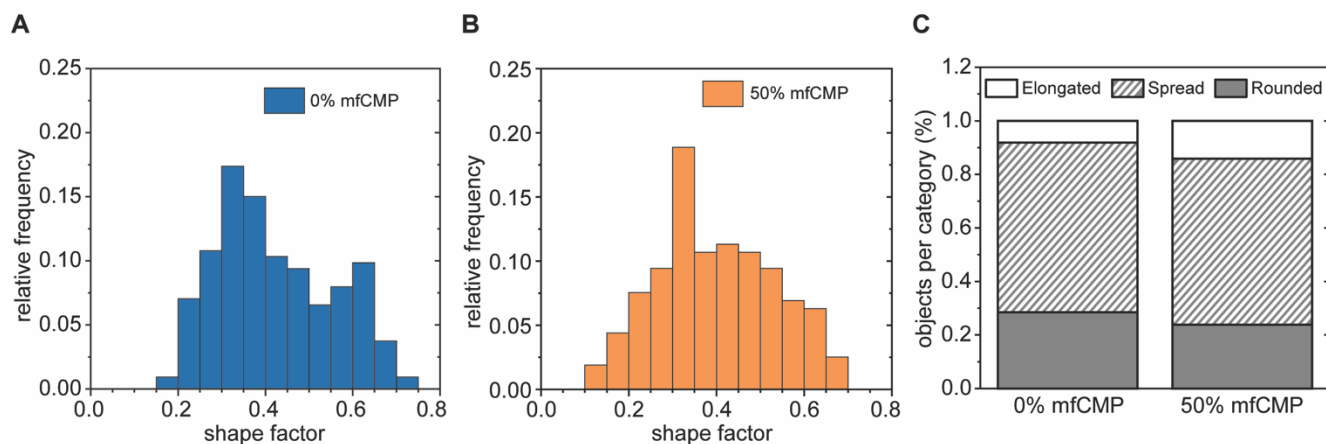


Figure S16: Impact of mfCMP-RGDS-PEG hydrogels on human lung fibroblast shape factor (sphericity). Using cytoskeletal and nuclear staining of fibroblasts after 6 days of culture within hydrogels (0% or 50% peptide linkages from mfCMP) (Figure 5A), cell morphology was analyzed. Here, the 3D shape factor (Ψ) of objects (individual cells or clusters of cells) was determined, where shape factor (a measurement of object sphericity) is defined by the equation: $\Psi = \frac{\pi^{1/3}(6V)^{2/3}}{A}$. (Ψ represents shape factor, V is the object volume, and A is the measured object surface area). The resulting shape factor values for each object are presented as histograms for hydrogels with (A) 0% mfCMP and (B) 50% mfCMP. (C) The shape factor data were then divided into three categories: *elongated* ($0 \leq \Psi \leq 0.25$), *spread* ($0.25 < \Psi \leq 0.5$), and *rounded* ($0.5 < \Psi \leq 1$) for comparison between hydrogel conditions. While there is a trend toward more elongated cells in the 50% mfCMP condition, there were no statistical differences in the percent of objects per category between the two hydrogel conditions.

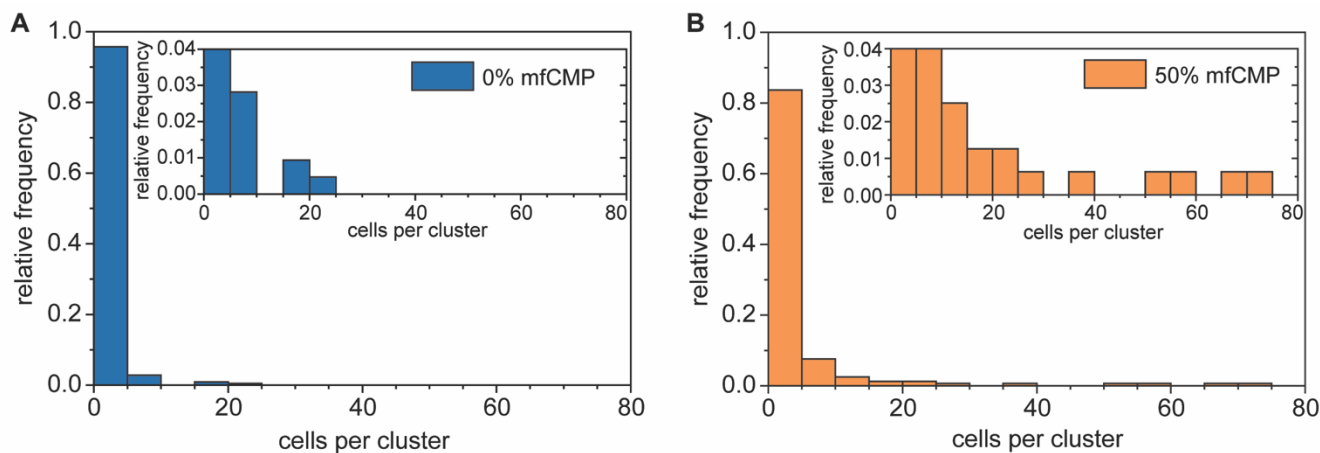


Figure S17: Number of cells per cluster of human lung fibroblasts in response to mfCMP-RGDS-PEG hydrogels. Histograms of the number of individual cells within each object for hydrogels with (A) 0% or (B) 50% of peptide linkages from mfCMP. These data were represented as half violin plots with individual data points in Figure 5C.

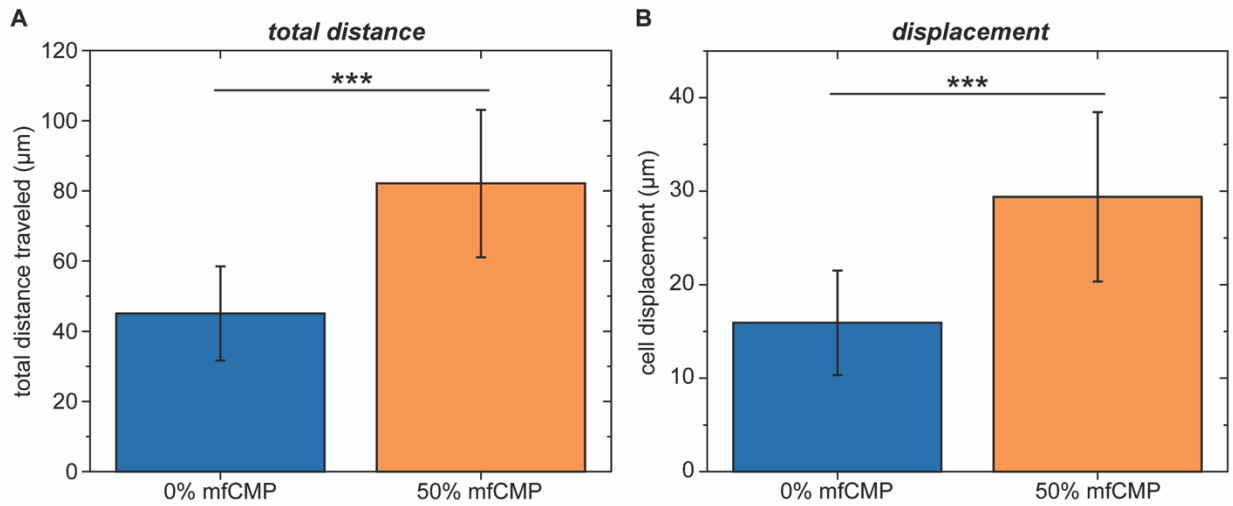


Figure S18: Total distance traveled and displacement of human lung fibroblasts in response to mfCMP-RGDS-PEG hydrogels. Fibroblasts were encapsulated within mfCMP-RGDS-PEG hydrogels (0% or 50% peptide linkages from mfCMP) and cell motility was monitored through timelapse imaging (24-36 hours after encapsulation). (A) Using timelapse imaging, each cell object (individual cells or clusters of cells) was tracked between frames to determine the total distance traveled (total distance, D). (B) The displacement (distance between the starting location and final position of each cell object, d) was also measured. (n = 3; *** p < 0.001.)

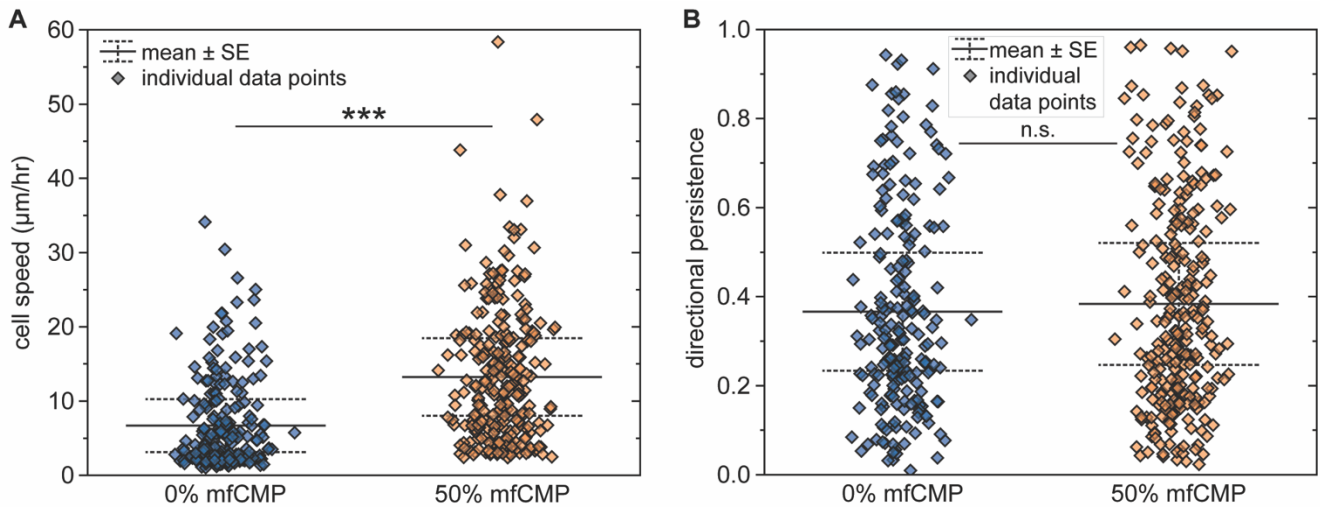


Figure S19: Impact of mfCMP-RGDS-PEG hydrogels on human lung fibroblast motility. Additional presentation of data from Figure 6B-C, where fibroblasts were encapsulated within mfCMP-RGDS-PEG hydrogels (0% or 50% peptide linkages from mfCMP) and cell motility was monitored from 24 hours to 36 hours after encapsulation. (A) Individual data points represent the speed of each cell object identified along with the mean \pm standard error. (B) Individual data points represent the directional persistence of each cell object identified along with the mean \pm standard error. Values closer to 0 indicate low directional persistence (meandering), where values closer to 1 indicate high directional persistence (direct movement). (***) p < 0.001; n.s. = means are not significantly different.)

Supplemental Tables

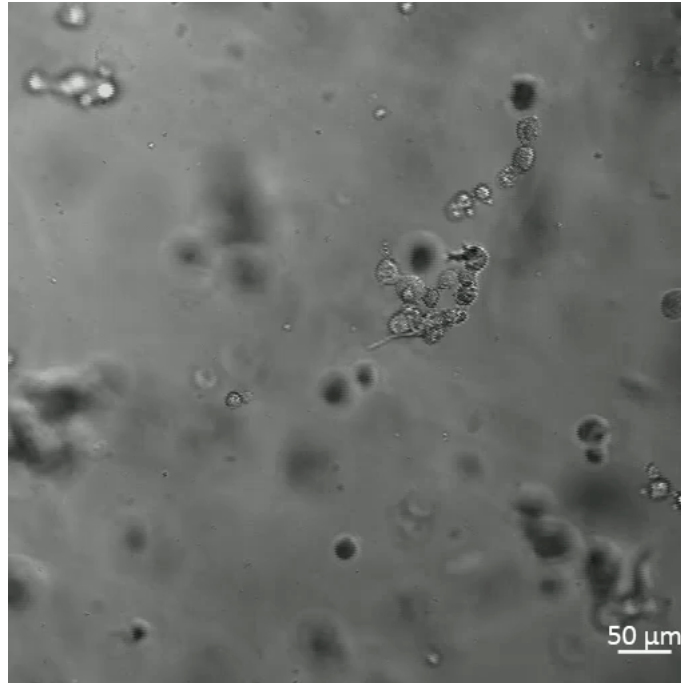
Table S1. mfCMP-PEG hydrogel formulations.

| | Functionality | 0% mfCMP 0 mM mfCMP (0% of peptide linkages) | 15% mfCMP 3 mM mfCMP (15% of peptide linkages) | 25% mfCMP 5 mM mfCMP (25% of peptide linkages) |
|---------------------------|---------------|--|--|--|
| PEG (mM thiol) | 4 | 20 | 20 | 20 |
| Linker Peptide (mM alloc) | 2 | 20 | 17 | 15 |
| mfCMP (mM alloc) | 1 | 0 | 3 | 5 |
| | Functionality | 35% mfCMP 7 mM mfCMP (35% of peptide linkages) | 50% mfCMP 10 mM mfCMP (50% of peptide linkages) | 75% mfCMP 15 mM mfCMP (75% of peptide linkages) |
| PEG (mM thiol) | 4 | 20 | 20 | 20 |
| Linker Peptide (mM alloc) | 2 | 13 | 10 | 5 |
| mfCMP (mM alloc) | 1 | 7 | 10 | 15 |
| | Functionality | 100% mfCMP 20 mM mfCMP (100% of peptide linkages) | | |
| PEG (mM thiol) | 4 | 20 | | |
| Linker Peptide (mM alloc) | 2 | 0 | | |
| mfCMP (mM alloc) | 1 | 20 | | |

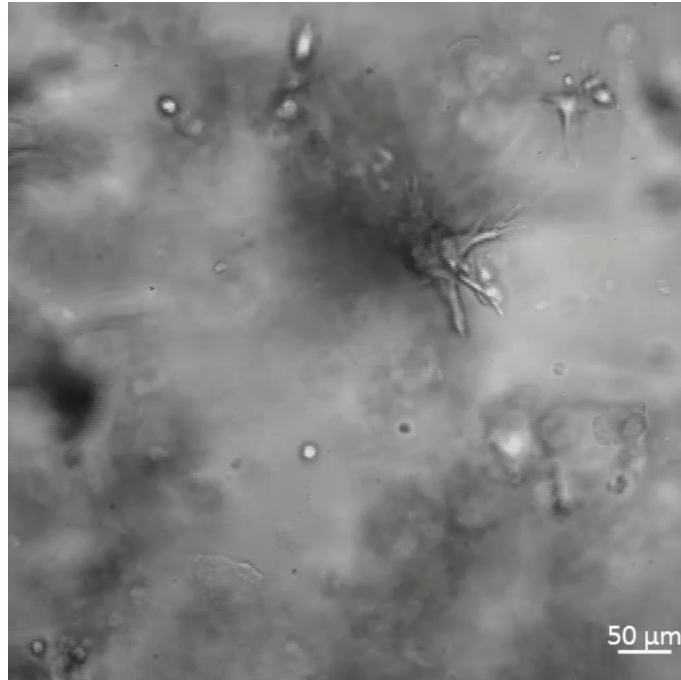
Table S2. mfCMP-RGDS-PEG hydrogel formulations for cell culture applications.

| | Functionality | 0 mM mfCMP <i>based on</i> 0% mfCMP (0% of total peptide linkages) | 5 mM mfCMP <i>based on</i> 25% mfCMP (32% of total peptide linkages) | 10 mM mfCMP <i>based on</i> 50% mfCMP (50% of total peptide linkages) |
|---------------------------|---------------|--|--|---|
| PEG (mM thiol) | 4 | 22 | 22 | 22 |
| Linker Peptide (mM alloc) | 2 | 11 | 10.5 | 10 |
| mfCMP (mM alloc) | 1 | 0 | 5 | 10 |
| RGDS (mM alloc) | 1 | 2 | 2 | 2 |
| Excess Thiol (mM) | | 9 | 4.5 | 0 |

Supplemental Videos



Video S1: Fibroblast motility in a 0% mfCMP hydrogel (0% of peptide linkages from mfCMP).
Video available online.



Video S2: Fibroblast motility in a 50% mfCMP hydrogel (50% of peptide linkages from mfCMP).
Video available online.